

## Research Article

# Shared Core Microbiome and Functionality of Key Taxa Suppressive to Banana Fusarium Wilt

Zongzhuan Shen <sup>1,2</sup>, Linda S. Thomashow,<sup>3</sup> Yannan Ou,<sup>1</sup> Chengyuan Tao,<sup>1</sup> Jiabao Wang,<sup>1,2</sup> Wu Xiong,<sup>1</sup> Hongjun Liu,<sup>1</sup> Rong Li,<sup>1,2</sup> Qirong Shen <sup>1,2</sup> and George A. Kowalchuk<sup>4</sup>

<sup>1</sup>Jiangsu Provincial Key Lab of Solid Organic Waste Utilization, Jiangsu Collaborative Innovation Center of Solid Organic Wastes, Educational Ministry Engineering Center of Resource-Saving Fertilizers, The Key Laboratory of Plant Immunity, Joint International Research Laboratory of Soil Health, Nanjing Agricultural University, Nanjing, 210095 Jiangsu, China

<sup>2</sup>The Sanya Institute of the Nanjing Agricultural University, Sanya, Hainan Province, China

<sup>3</sup>U.S. Department of Agriculture, Agricultural Research Service, Wheat Health, Genetics and Quality Research Unit, Pullman, WA, USA

<sup>4</sup>Ecology and Biodiversity Group, Institute of Environmental Biology, Department of Biology, Utrecht University, 3584 CH Utrecht, Netherlands

Correspondence should be addressed to Qirong Shen; qirongshen@njau.edu.cn

Received 31 March 2022; Accepted 22 August 2022; Published 16 September 2022

Copyright © 2022 Zongzhuan Shen et al. Exclusive Licensee Science and Technology Review Publishing House. Distributed under a Creative Commons Attribution License (CC BY 4.0).

Microbial contributions to natural soil suppressiveness have been reported for a range of plant pathogens and cropping systems. To disentangle the mechanisms underlying suppression of banana Panama disease caused by *Fusarium oxysporum* f. sp. *cubense* tropical race 4 (Foc4), we used amplicon sequencing to analyze the composition of the soil microbiome from six separate locations, each comprised of paired orchards, one potentially suppressive and one conducive to the disease. Functional potentials of the microbiomes from one site were further examined by shotgun metagenomic sequencing after soil suppressiveness was confirmed by greenhouse experiments. Potential key antagonists involved in disease suppression were also isolated, and their activities were validated by a combination of microcosm and pot experiments. We found that potentially suppressive soils shared a common core community with relatively low levels of *F. oxysporum* and relatively high proportions of Myxococcales, Pseudomonadales, and Xanthomonadales, with five genera, *Anaeromyxobacter*, *Kofleria*, *Plesiocystis*, *Pseudomonas*, and *Rhodanobacter* being significantly enriched. Further, *Pseudomonas* was identified as a potential key taxon linked to pathogen suppression. Metagenomic analysis showed that, compared to the conducive soil, the microbiome in the disease suppressive soil displayed a significantly greater incidence of genes related to quorum sensing, biofilm formation, and synthesis of antimicrobial compounds potentially active against Foc4. We also recovered a higher frequency of antagonistic *Pseudomonas* isolates from disease suppressive experimental field sites, and their protective effects against banana *Fusarium* wilt disease were demonstrated under greenhouse conditions. Despite differences in location and soil conditions, separately located suppressive soils shared common characteristics, including enrichment of Myxococcales, Pseudomonadales, and Xanthomonadales, and enrichment of specific *Pseudomonas* populations with antagonistic activity against the pathogen. Moreover, changes in functional capacity toward an increase in quorum sensing, biofilm formation, and antimicrobial compound synthesizing involve in disease suppression.

## 1. Introduction

Soil-borne diseases can severely impact global crop production across a wide range of crops, cropping systems and disease-causing agent, and these impacts are expected

to increase under conditions of climate change [1]. Plant diseases are estimated to be responsible for as many as twenty percent of global food production lost annually [2]. As one of the most devastating soil-borne pathogens across many agricultural production systems in the world, *Fusarium*

spp. could attack a range of important crops resulting in damping-off, root rot, and vascular wilt [3]. Banana *Fusarium* wilt, also known as Panama disease, was caused by the infection of *Fusarium oxysporum* f. sp. cubense tropical race 4 (Foc4) [4]. This *Fusarium* wilt is notably hard to control, probably due to the pathogen which could produce chlamydospores that can survive in soil for decades [5]. Plant root-associated microbiomes are increasingly recognized as a possible dominator of natural pathogen suppression and have become a goal for innovative ways aimed at improving disease management [6]. Despite evidence that many bio-control agents can contribute to relieving the damage caused by *Fusarium* wilt [7], a main problem is that their efficacy is unstable under field conditions. Therefore, it is important for us to improve our ability in predicting and engineering microbiome functions to increase soil suppressiveness.

Disease-suppressive soil is the best evidence that illustrating microorganisms participated in the plant protection against soil-borne pathogens. Disease-suppressive soil has been defined as those in which disease incidence or severity still maintains at a low level, even in the presence of the pathogen, susceptible host crop, and climatic condition conducive to disease occurrence [8]. With the understanding of the necessity to reduce the application of chemical pesticides, suppressive soil has emerged as a research hotspot with important implications in the development of more sustainable agriculture [9]. Disease-suppressive soil could provide a basis for manipulating soil community to generate sustainable alternate strategies for pathogen control, and soils suppressive to soil-borne pathogens have been discovered for a range of crops across many locations [10–12]. Although banana-suppressive soils to *Fusarium* wilt have previously been reported [13–15], it is still challenging to unravel the complicated microbial mechanisms with regard to disease suppression.

With the development of DNA sequencing techniques, it has become more feasible to describe the microbial consortia potentially responsible for disease suppression across a range of pathosystems [16]. The rhizosphere represents the zone of interaction between the soil microorganisms and plant roots, and it has therefore been the focus of studies relating soil-borne communities to disease suppressive capacities [9, 10, 17]. Such studies have typically examined specific natural disease-suppressive soils, attributing disease-suppressive properties to the presence of specific antagonistic microorganisms, such as *Burkholderia* [18], *Lysobacter* [17], and *Streptomyces* [9]. However, soil communities are known to vary greatly across sites determined by a range of abiotic and biotic factors [19]. It is generally unknown whether there are common features of disease-suppressive soils against target pathogens across agricultural fields that differ in location and edaphic factors.

To expand our understanding about the general microbial properties of disease-suppressive soils, we aimed to (1) investigate whether separately located disease-suppressive agricultural soils shared common microbial community features, (2) identify keystone microbial groups potentially involved in disease suppression across different field sites, and (3) verify the ability of identified keystone microbes to suppress *Fusarium* wilt disease. With these goals in mind,

the microbiome across six agricultural sites under long-term monocropping of banana in Hainan Island, China, was examined (Figure 1(a)). Each site included paired orchards, one potentially suppressive to banana wilt and the other conducive to the disease. We used both community-based sequencing and classical approaches to decipher the geographically distributed *Fusarium* wilt-suppressive soils. Common features of disease-suppressive soil were first used to identify microbial taxa potentially involved in disease suppression, and subsequent cultivation-based microcosm experiments were used to assess the potential of some of these taxa to suppress the pathogen. In total, we sought to reveal how core features of the soil microbiome may impact pathogen suppression across a range of field conditions and sites.

## 2. Results

**2.1. Soil Properties and Microbial Biomass.** Potentially disease-suppressive soils from the six geographically separated banana orchards differed in their soil properties and edaphic factors (Table S1). However, in comparison to the disease-conductive soils, disease-suppressive soils exhibited a higher pH and higher contents of available phosphorus (AP), available potassium (AK), total carbon (TOC), and total nitrogen (TON) on average. Although the differences in bacterial and fungal abundances were not significant, disease-suppressive soils together showed significantly higher ratios of bacteria to fungi (*B/F*) compared to disease-conductive soils based on quantitative PCR assays (Figure S1). Furthermore, disease-suppressive soils together harbored a significantly lower abundance of Foc4 compared to disease-conductive soils (Figure 1(b)).

**2.2. Shared Core Microbiome Features across Disease-Suppressive Soils.** Amplicon sequencing resulted in 8,075 bacterial and 2,844 fungal OTUs in total across all disease-suppressive and -conductive soils based on 97% similarity after basic quality control (Figure 1(c)). The rarefaction curves for each sample nearly approached saturation, indicating that the sequencing data were reasonable for evaluating the microbial diversity and composition (Figure S2). Given many rare taxa only detected in specific locations, we further sought to examine features of the core microbiome across all sites. OTUs that appear as in at least 80% of all soil samples were defined as belonging to the core microbiome. A total of 1,033 bacterial OTUs sequences and 92 fungal OTUs were deemed to constitute the core microbiomes for pooled disease suppressive and conducive soils (Figure 1(c), Table S2). No significant difference was observed for Shannon index of core bacterial and fungal communities (Figure S3). The core bacterial microbiome consists of Acidobacteria, Actinobacteria, Bacteroidetes, Firmicutes, Gemmatimonadetes, Proteobacteria, and other low relative abundance phyla while the core fungal microbiome was mainly comprised by Ascomycota, Basidiomycota, Glomeromycota, and Zygomycota both in the potentially conducive and suppressive soils (Figure S4).

Nonmetric multidimensional scaling ordination (NMDS) analysis exhibited distinct differences in the

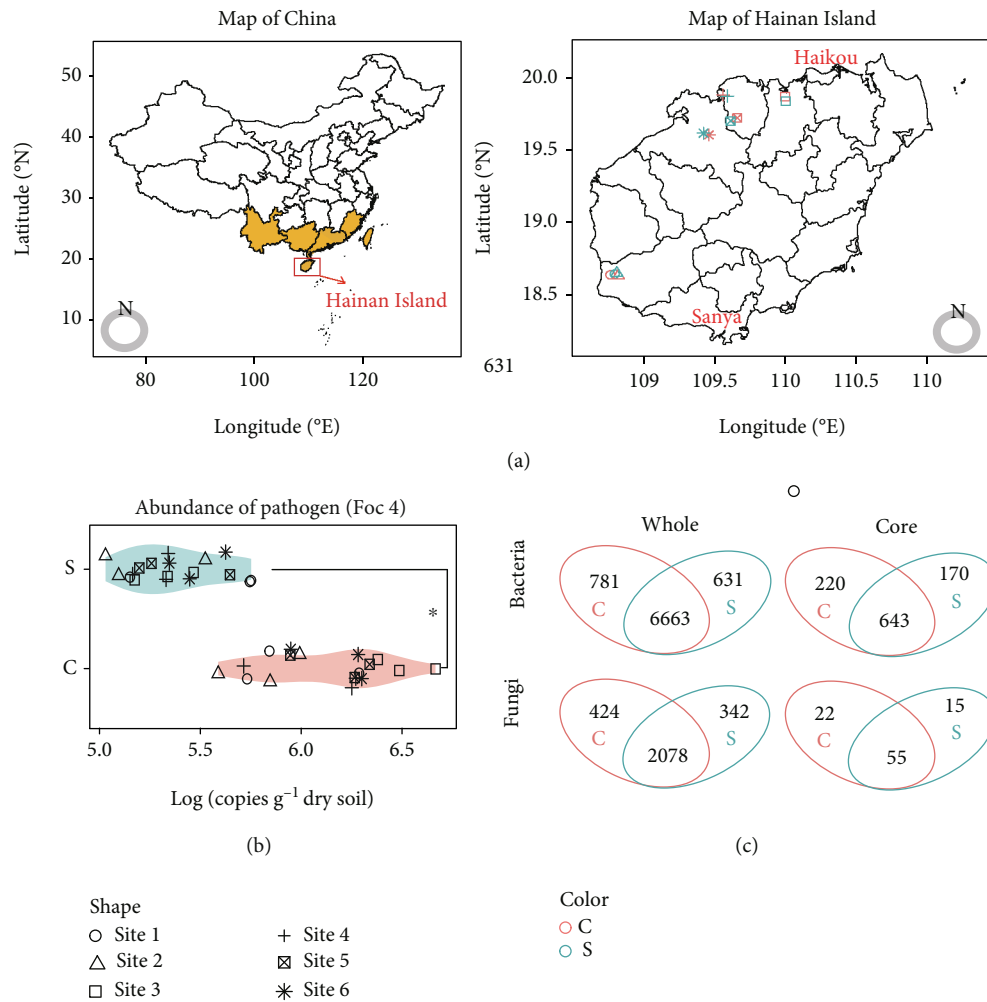


FIGURE 1: Distribution of soil sampling sites and overview of the composition of the core bacterial and fungal communities. (a) Map showing the location of selected orchards. Yellow areas represent the main banana production regions in China. (b) Violin plot depicting the mean abundance of Foc4 in disease-suppressive (S) and -conductive (C) soils. The \* indicates a significant difference between C and S orchards according to Wilcoxon tests. (c) Venn diagram exhibiting the unique and shared bacterial and fungal OTUs between conducive and suppressive orchards for the total and core microbiomes.  $C_{\text{whole}}$  and  $S_{\text{whole}}$  represent all identified OTUs within the microbiome, while  $C_{\text{core}}$  and  $S_{\text{core}}$  represent OTUs designated as being part of the core microbiome.

composition of bacterial and fungal community with respect to site location site and disease-suppressive ability. Using the full bacterial and fungal community datasets, field location was found to be the first factor distinguishing microbial community structure (Figure 2(a), Table S3). However, when only considering the core communities, core bacterial communities from disease-suppressive soils were grouped together, with a clear separation from those of the disease-conductive soils (Figure 2(b), Table S3). Despite both location and suppressive ability were significant drivers for total and core bacterial and fungal communities, however, location was more important for total communities while suppressive ability was more so for the core communities, especially for bacterial communities.

**2.3. Potential Key Species within Shared Core Microbiomes of Disease-Suppressive Soils.** Among the dominant phyla of core bacterial communities, a significantly higher relative abundance of Proteobacteria and lower relative abundance

of Acidobacteria on average were observed in potentially suppressive soils (Figure 3(a), Table S4). Further, the results of relative change analysis displayed that Proteobacteria were only significantly enriched in disease-suppressive soils (Figure 3(b)). Within the Proteobacteria, the Myxococcales, Pseudomonadales, and Xanthomonadales showed significantly higher relative abundance in suppressive soils as compared to conducive soils when examining relative changes at the order level (Figure 3(b), Table S5). Within these three enriched orders, five genera, *Anaeromyxobacter*, *Kofleria*, *Plesiocystis*, *Pseudomonas*, and *Rhodanobacter*, were found to be significantly enriched in disease-suppressive soils as compared to conducive soils (Figure S5). Further, random forest analysis showed that the enrichment of *Pseudomonas* in potentially disease-suppressive soils was the most important variable for predicting the reduced abundance of Foc4 among these five genera (Figure 3(c)). Moreover, quantitative PCR results showed that potentially disease-suppressive soils contained higher abundances of *Pseudomonas* than disease-conductive

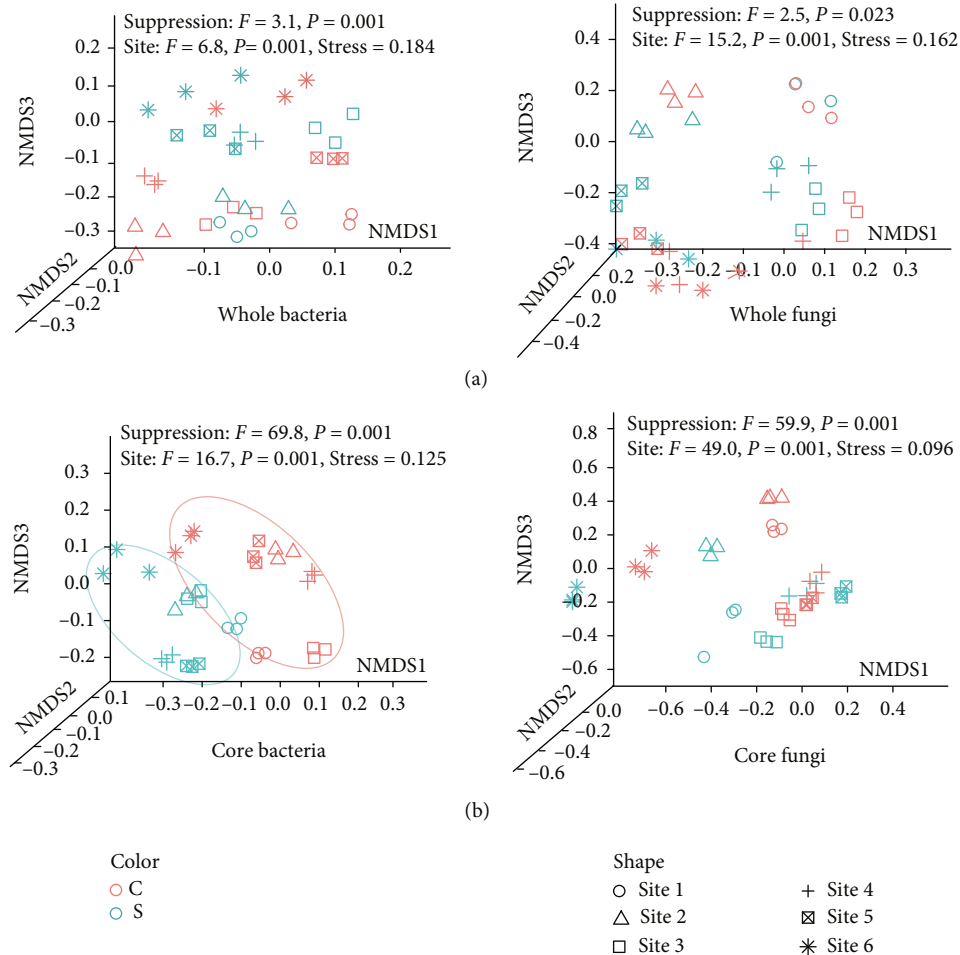


FIGURE 2: Structure of whole and core microbiome in disease-suppressive and -conductive soils. (a) Nonmetric multidimensional scaling (NMDS) ordination plots displaying the composition differences for whole bacterial and fungal community calculated using weighted UniFrac distances. (b) NMDS plot displaying the composition differences for core bacterial and fungal community calculated using weighted UniFrac distances.

soils (Figure 3(d)). In addition, potentially suppressive soils harbored a significantly lower relative abundance of *F. oxysporum* on average (Figure 3(e)).

**2.4. Transfer of Disease Suppressiveness.** A low level of disease incidence was observed when banana plants were grown in disease-suppressive soil even inoculated with Foc4 under greenhouse conditions. In contrast, nearly all plants became diseased when conducive soils were amended with a Foc4 spore suspension (Figure 4(a)). Further, disease suppressiveness of the disease-suppressive soil was partially lost when the soil was heated to 50°C. In soil-transfer experiments, in which 10% of suppressive soil was mixed with conducive soil before plant cultivation, disease suppressiveness was partially transferred (Figure 4(b)). Collectively, these results support the notion that observed disease suppressiveness toward Foc4 is biological in nature.

**2.5. Functional Traits of the Soil Microbiome in Disease-Suppressive Soil.** Shotgun sequencing of the disease-suppressive and -conductive soils from the experimental field site 3 resulted in an average of 17.2 GB paired-end reads per

sample, totaling 172 GB high-quality reads after quality control (Table S6). The filtered sequences were de novo assembled to yield an average of 114,849 contigs, and an average of 176,417 ORFs was generated for each sample (Table S7). When the final sequences were blasted against the COG database, a higher fraction of pathways related to the biosynthesis of secondary metabolites was found in the suppressive soil as compared to conducive soil. When blasting DNA reads against the KEGG database, a higher frequency of pathways involved in quorum sensing and biofilm formation was observed in the disease-suppressive soil (Figure 4(c)). Taxonomic assignment of the annotated DNA reads also identified members of *Pseudomonas* as more abundant in the disease-suppressive soil as compared to the conducive soil (Figure 4(d)). NMDS analysis was also performed on functional genes related to *Pseudomonas* as determined using the PHI database, revealing a clear distinction in *Pseudomonas* functional traits that was observed between disease-suppressive and -conductive soils (Figure 4(e)). Interestingly, genes involved in “unaffected pathogenicity” and “effector of plant virulence determinants” were significantly depleted in the suppressive soil, and genes

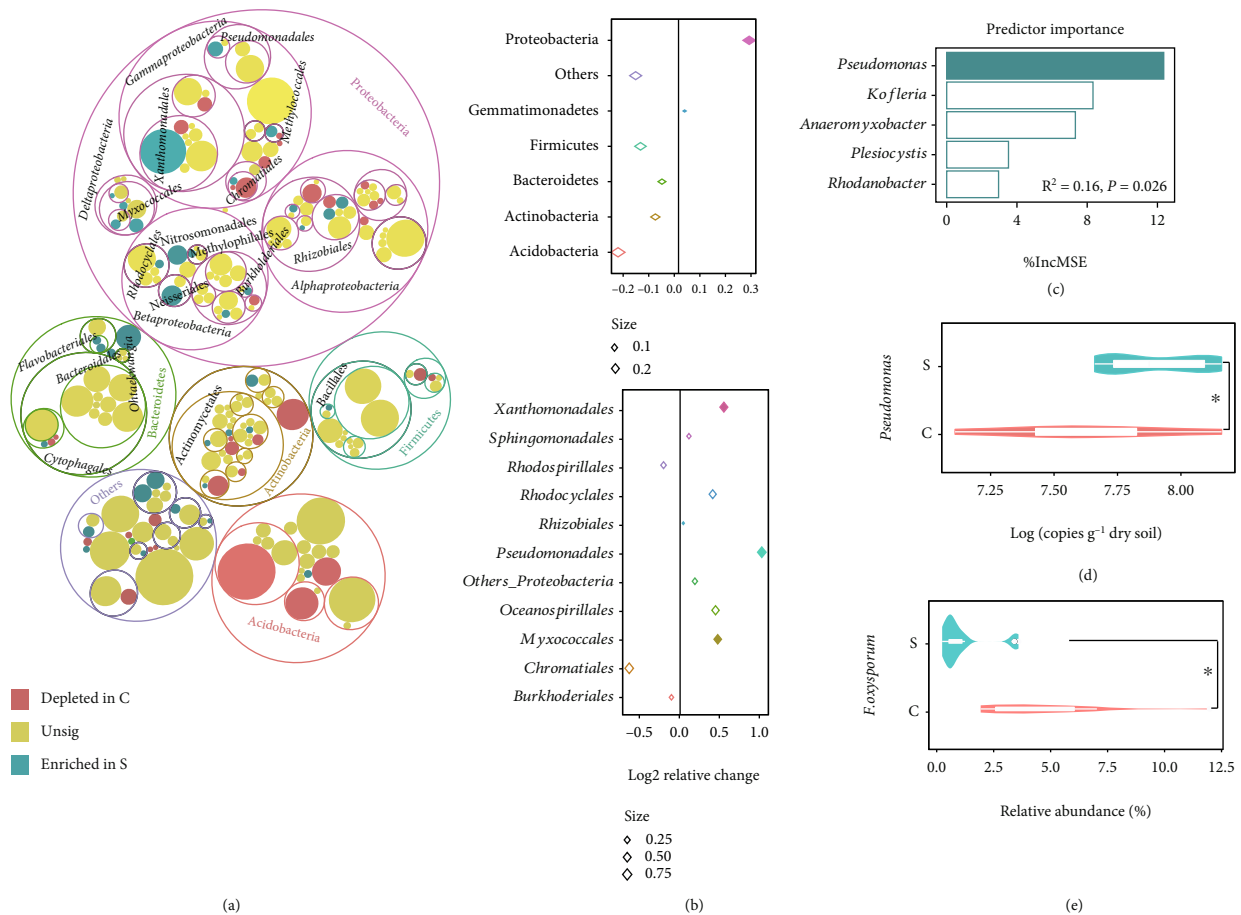


FIGURE 3: Key taxa for the core microbiome in disease-suppressive soils. (a) Taxonomic differences for the core bacterial microbiome between disease-suppressive and -conductive soils are based on 16S rRNA gene sequences. The outside circles to inner circles represent phylum, class, order, and family level, respectively. Solid circles represent genera. (b) Bubble graph showing the log<sub>2</sub> transformed relative changes of dominate phyla and orders in significantly enriched phylum of Proteobacteria in disease suppressive to conducive soils for core bacterial community. Rhombus size indicates absolute value of the log<sub>2</sub> transformed relative changes. Solid rhombus indicates that the taxa were significantly enriched in disease-suppressive soils. (c) Random forest mean predictor importance of relative abundance of significantly enriched genera among the Myxococcales, Pseudomonadales, and Xanthomonadales as drivers for the abundance of Foc4 in soil. Solid bar represents that the specific predictor is significant. MSE: mean square error. (d) Violin plot showing the abundance of *Pseudomonas* in disease-suppressive (S) and -conductive (C) soils. The \* indicates a significant difference between C and S treatments based on Wilcoxon tests. (e) Violin plot showing the relative abundance of *F. oxysporum* in the core microbiome in disease-suppressive and -conductive soils. The \* indicates a significant difference between C and S treatments based on Wilcoxon tests.

related to reduced virulence were significantly enriched in these samples (Figure 4(f)). A further secondary metabolite analysis by using antiSMASH exhibited that NRPS was significantly enriched in the disease-suppressive soil compared to disease-conductive soil (Figure 4(g)).

**2.6. *Pseudomonas* Isolates from Disease-Suppressive Soils and Their Abilities to Suppress *Foc4* Invasion.** Although the counts of culturable bacteria between disease-conductive and -suppressive soils were not significantly differed, disease-suppressive soils exhibited higher counts of culturable *Pseudomonas* compared to conducive soils (Figure 5(a)). Results of dual culture assays revealed that only 6.4% of isolated *Pseudomonas* strains were antagonistic to the *Foc4*, with 56 antagonistic strains recovered from disease suppressive soils and 37 strains from conducive soils (Figure 5(a)). Subsequently, four antagonistic *Pseudomonas* strains S9, S20, S27, and S40 from disease-

suppressive soils were selected for further analysis based upon the fact that they exhibited the largest inhibition zones (>10 mm) (Figure 5(b)).

A greenhouse experiment showed that the application of each of these four antagonistic *Pseudomonas* strains to field soil could significantly decreased the incidence of banana *Fusarium* wilt three months after seedlings were transplanted. Compared to controls without introduced *Pseudomonas* strains (CK), treatment (T5) with the mixture of fermentation cultures from these four antagonistic *Pseudomonas* strains displayed the lowest disease incidence, with a 39.4% decrease of disease (Figure 6(a)). Quantitative PCR results showed that all treatments amended with antagonistic *Pseudomonas* strains displayed reduced abundance of *F. oxysporum* in the banana rhizosphere soil compared to the CK treatment (Figure 6(b)). Also, treatments T1, T3, T4, and T5 exhibited a greater abundance of *Pseudomonas* in the

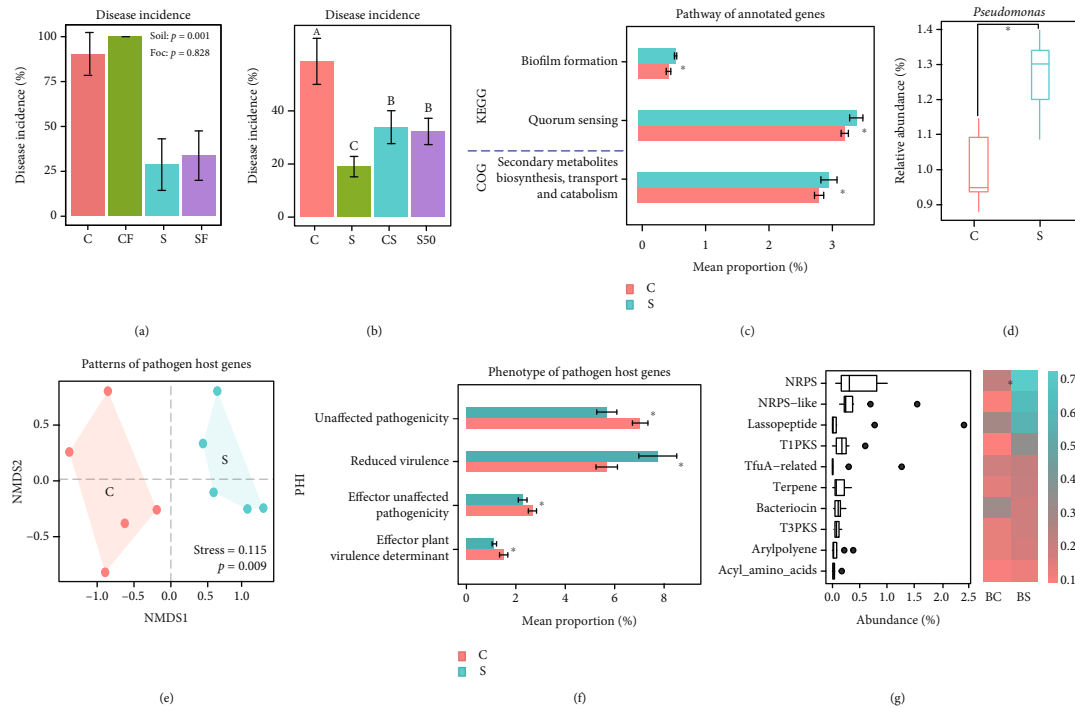


FIGURE 4: Functionalities in disease-suppressive and -conductive soils. (a) Histogram showing the percentage (mean  $\pm$  standard error of four replicates) of banana tissue seedlings with *Fusarium* wilt symptoms in conducive soil (C), conducive soil inoculated with Foc4 (CF), suppressive soil (S), and suppressive soil inoculated with Foc4 (SF). (b) Histogram showing the percentage of banana tissue seedlings with *Fusarium* wilt symptoms in conducive soil (C), suppressive soil (S), conducive soil mixed with 10% (w/w) suppressive soil (CS), or suppressive soil heated to 50°C (S50). Different letters above the bars mean significant differences ( $p < 0.05$ , ANOVA test). (c) Pathways that are significantly enriched in banana orchards suppressive to *Fusarium* wilt when metagenome sequences were blasted against KEGG and COG databases. The \* above the bar represents a significant difference between C and S treatments based on ANOVA test. (d) Boxplot showing the relative abundance of *Pseudomonas* in soils suppressive or conducive to *Fusarium* wilt as final metagenomic dataset blasted against the NR database. (e) NMDS ordination plot displaying the functional differences between suppressive and conducive soils based on metagenomic analysis of genes related to the *Pseudomonas* community when blasted against the PHI database. (f) Bar plot showing the phenotypic differences between suppressive and conducive soils according to metagenomic analysis of genes related to the *Pseudomonas* community when blasted against the PHI database. (g) The boxplot in the left panel displaying the top 10 abundant secondary metabolites in the soils on average based on the antiSMASH database. The heatmap in the right panel showing the top 10 abundant secondary metabolites related to antimicrobial compounds synthesizing in the disease conducive (C) and suppressive (S) soils. The heatmap was plotted according to the mean intensity, and the \* in the heatmap cell symbol indicates a significant difference between C and S treatments.

rhizosphere compared to the CK treatment (Figure 6(c)). These results resulted in a significantly negative correlation between the abundance of *Pseudomonas* and *F. oxysporum* in the banana rhizosphere soil of this experiment (Figure 6(d)).

### 3. Discussion

The diversity of plant and microbiome in natural ecosystems can help maintain low levels of disease [20], but the intensive agriculture that continuously growing with a little number of crop varieties leads to an outbreak of soil-borne diseases caused by plant pathogens. With consecutive cropping of the same crop cultivar or application of soil amendments, monocropped soils can achieve disease suppression as a result of the selection and enrichment of antagonistic microorganisms or overall microbial diversity that can suppress the soil-borne pathogen [21]. Previous studies have often been confined to the examination of microbial

composition in disease-suppressive soils of specific crops from a single site. However, different fields of the same cropping system can vary greatly in their soil characteristics and hence overall soil-borne microbial community composition [22, 23]. Thus, we still have a relatively limited understanding of whether signatures of suppressive soils are held in common across different field sites. The microbial compositions in *Fusarium* wilt-diseased and disease-free banana orchards have been explored previously [24, 25]; however, this is the first study that attempts to investigate whether geographically distributed agricultural soils suppressive to *Fusarium* wilt exhibit community features that can be connected with their disease-suppressive capacities.

In the current study, NMDS of the full bacterial and fungal communities across the different sites revealed that the location site was the dominating driver of microbial community patterns. This observation is in line with previous reports that soil characteristics and large-scale distribution

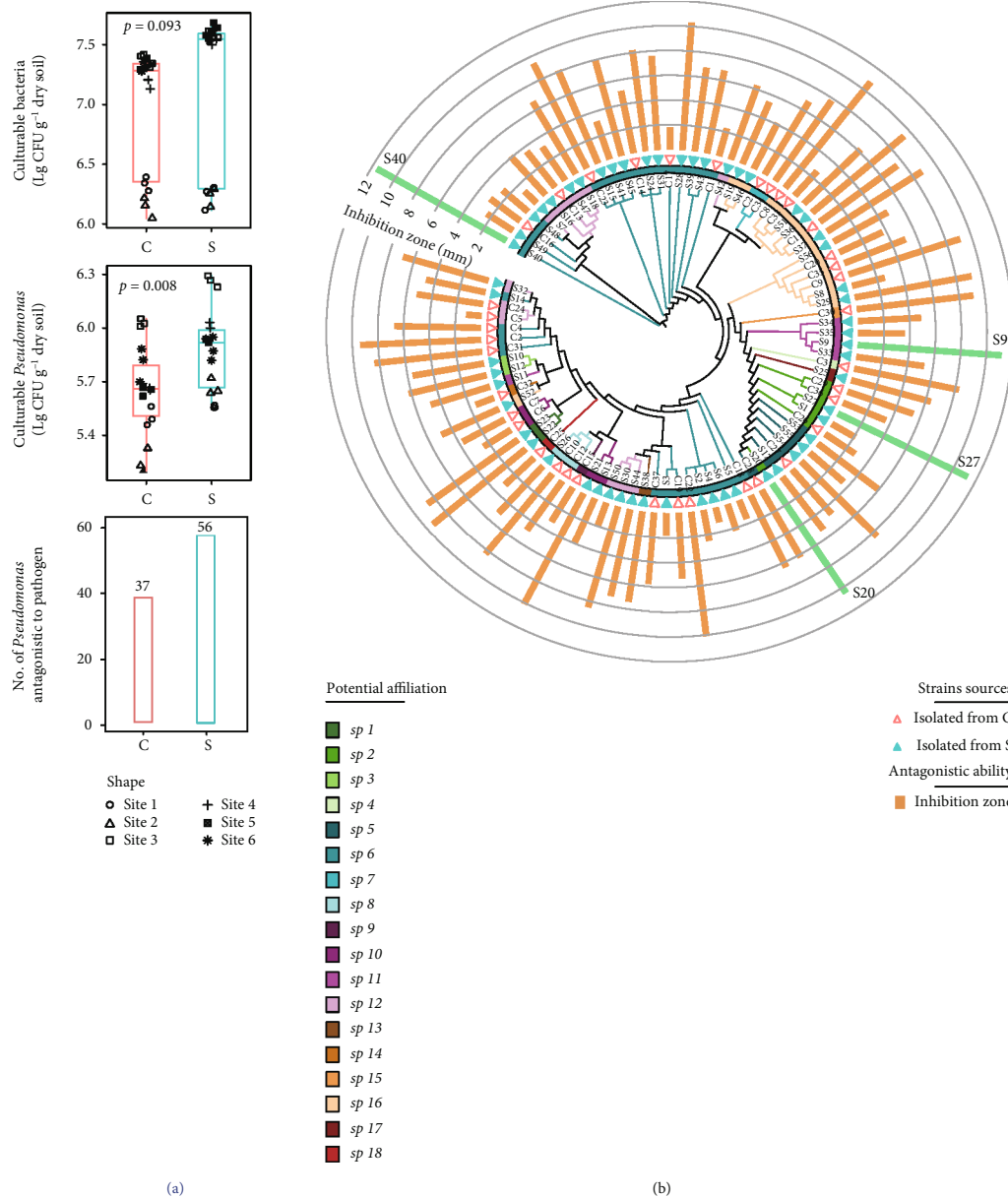


FIGURE 5: Isolation and identification of antagonistic *Pseudomonas* spp. in disease-suppressive and -conductive soils. (a) Histogram exhibiting the culturable counts of bacteria and *Pseudomonas* in conducive (C) and suppressive (S) soil, and the number of antagonistic *Pseudomonas* antagonistic to *Foc4* isolated from C and S field soils. (b) Cladogram depicting potential phylogenetic relationships between isolated *Pseudomonas* strains in disease-suppressive or -conductive soils. Leaf labels are representative IDs of each strain. The inner rings indicate the potential species-level taxonomy according to 16S rRNA genes, and the outer ring represents the soil from which the strain was isolated. The bar plot above each node represents the antagonistic ability against *Foc4*. The length of each bar was plotted based on the inhibition zone of the *Pseudomonas* strain against *Foc4*. Solid and empty triangles represent the strains isolated from C or S treatments, respectively.

patterns are the principal drivers of total community structure in soil [26, 27]. However, when considering the core microbiome, consisting of 1,033 bacterial OTUs and 92 fungal OTUs, we found disease-suppressive capacity to be a major determinant of the community structure. This finding is consistent with the notion that key characteristics of the core rhizosphere microbiome can develop independently of larger course-scale environmental drivers [28]. Core microbiomes were recently proposed as sets of microbial taxa that play similar functions at the ecosystem level, and they have

been recognized across a range of various environmental factors [29]. The soils suppressive to banana *Fusarium* wilt disease across a range of locations shared feature of their core microbial community, suggesting that disease suppressive soils may involve the selection of a set of ubiquitous microbial species involved in disease suppression under the stress of pathogen invasion.

Similar to other studies using community-based analyses of core bacterial soil communities [30–32], the core bacteria taxa in our study were dominated by Acidobacteria,

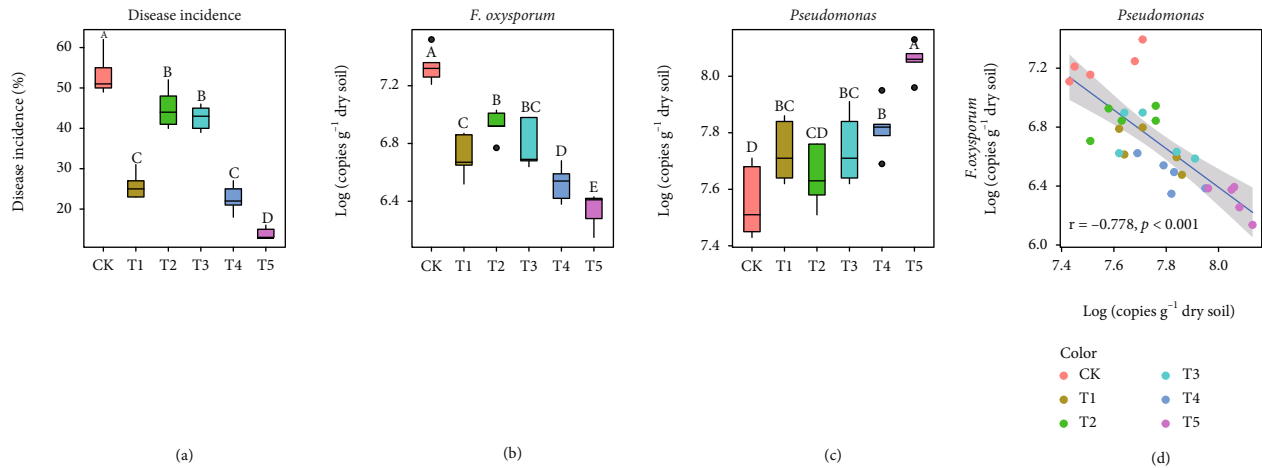


FIGURE 6: Effects of selected antagonistic *Pseudomonas* spp. on disease suppression. (a) Boxplot showing the disease incidence of different treatments amended with different antagonistic *Pseudomonas* isolates. Different letters above the boxes indicate statistically significant differences (ANOVA,  $p < 0.05$ ). Treatments of T1, T2, T3, and T4 represent monocropped soil amended with 50 mL fermentation liquor of the *Pseudomonas* strains S9, S20, S27, and S40, respectively. T5 represents monocropped soil amended with 50 mL equally mixed fermentation liquors from all above four strains (T5). CK represents control of monocropped soil amended with 50 mL sterile KB broth. (b) Boxplot showing the abundance of *F. oxysporum* in the rhizosphere soils from different treatments. (c) Boxplot showing the abundance of *Pseudomonas* in the rhizosphere soils from different treatments. (d) Scatter diagram depicting the correlations between the relative abundance of *Pseudomonas* and the abundance of *F. oxysporum* in the rhizosphere soils.

Actinobacteria, Bacteroidetes, Firmicutes, Gemmatimonadetes, and Proteobacteria. Although no other reports have been focused on core fungal communities, the core fungal community was mainly comprised by Ascomycota, Basidiomycota, Glomeromycota, and Zygomycota in our study. Our results suggest that the core microbiome of these wilt-suppressive soils contains fundamental taxonomic groups probably involved in supporting basic soil functions [33–35].

As previously found in studies of banana Panama disease [36], disease-suppressive soils had lower proportion of *F. oxysporum* as compared to the disease-conducive soils. Our results demonstrated that Proteobacteria in the core bacterial community are significantly enriched in banana soils suppressive to banana Panama disease, which is in agreement with previous studies suggesting that members of the gamma-proteobacteria can be considered as keystone species of healthy banana plants in *Fusarium* wilt-infested orchards [37, 38]. We further found that the relative abundances of Myxococcales, Pseudomonadales, and Xanthomonadales within the Proteobacteria were significantly increased in disease-suppressive soils. As many isolates from these three orders were considered as the most promising biocontrol agents [39, 40], our results suggest that members of Myxococcales, Pseudomonadales, and Xanthomonadales may be involved in maintaining the soil suppressiveness to banana *Fusarium* wilt.

The culture-independent approaches employed in this study, including random forest analysis based on amplicon sequencing results and taxonomic analysis of shotgun sequencing results, showed that *Pseudomonas* may play crucial roles in determining soil suppressiveness of soils suppressive to banana Panama disease. Furthermore, culture-dependent analyses demonstrated that isolates of *Pseudomonas* from suppressive soils with the capacity to suppress the

growth of Foc4 could protect banana from pathogen invasion. *Pseudomonas* populations have constantly been recognized to be involved in the suppression of *Fusarium* wilt disease or wheat take-all disease [41, 42], as well as playing a vital role against pathogen infection in the banana endophytic microbiome [43]. One possible mechanism behind wilt suppression may be the production of antimicrobial compounds [44]. In agreement with this, we found that the microbiome in disease-suppressive soils had a higher proportion of functional genes linked to the biosynthesis of secondary metabolites. Another possible mechanism could be the occupation of niches overlapping with the pathogen thereby leading to competition for instance for available resources [45]. It was reported that beneficial microbes may preferentially colonize the root niches and compete available resources via formatting biofilm to suppress the pathogen invasion [46]. In line with this, we observed that disease-suppressive soils displayed a higher frequency of functional genes relating to biofilm formation. Both biofilm formation and the production of many antibiotics by gram-negative bacteria are linked to quorum sensing [47, 48]. Interestingly, we also found higher frequencies of genes for quorum sensing in our suppressive soils, indicating that it likely plays a key role in suppressing pathogen invasion.

Notably, despite the high population size of *Pseudomonas* in disease suppressive as compared to conducive soils, only a small percentage of *Pseudomonas* isolates with antagonistic activity *in vitro* were recovered in the present study, in agreement with a previous report that not all *Pseudomonas* spp. isolates directly inhibit pathogens [49]. Although more antagonistic *Pseudomonas* isolates were found in the suppressive than in the conducive soils, the quorum sensing and biofilm of *Pseudomonas* probably contribute to the soil suppressiveness as well. Hence, we suggest that *Pseudomonas*



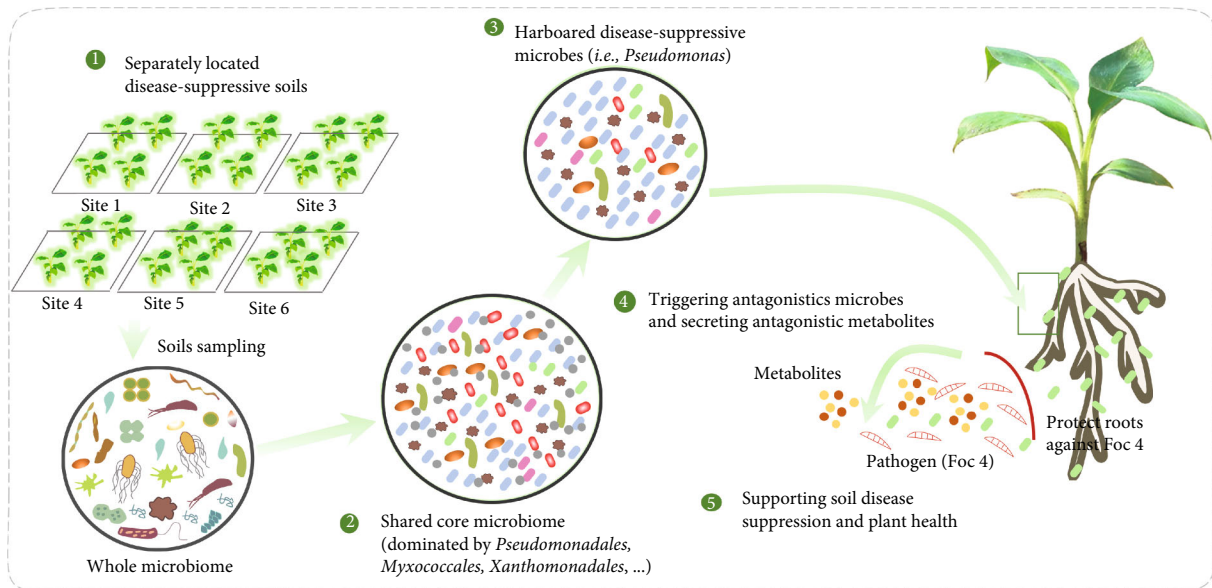


FIGURE 7: Conceptual model illustrating the shared core microbiome and potential mechanism in separately located disease-suppressive soils. Picture summarizing the features of core microbiome in separately located disease-suppressive soils and potential mechanism of disease-suppressive microbes against fungal pathogen growth and subsequent plant infection.

spp. in the suppressive soil were stimulated under the pressure of the pathogen and by interactions with the indigenous microbiome. In agreement with this hypothesis, a clear difference in pathogenicity and virulence of *Pseudomonas* communities was observed in our study, generally supporting the idea that the function of the microbiome is redundant and probably can be directed in specific directions under biotic or abiotic stress [50].

Thus, by combining cultivation-dependent and independent approaches, we were able to identify that *Pseudomonas* has a key group in the activity of the core microbiome of these disparately located disease-suppressive soils. However, other taxa are mostly likely also involved, given the fact that soil suppressiveness is often governed by the combined activities of microbial consortia [51]. In our study, we also observed heightened levels of the Myxococcales and Xanthomonadales in disease-suppressive soils, and members of these groups merit further investigation for their potential roles in the control of Foc4. Also, we focused primarily on strains that showed antagonistic activities in monoculture, and it is known that many antagonistic activities are the product of interactions of strains often showing no direct individual effects [52].

In conclusion, by examining six separate field locations, each with paired orchards either suppressive or conducive to *Fusarium* wilt, we were able to identify consistent microbiome signatures related to disease suppressiveness (Figure 7). Disease-suppressive soils exhibited a higher relative abundance of Myxococcales, Pseudomonadales, and Xanthomonadales. Metagenomic analysis of one pair of adjacent orchards also showed that the disease-suppressive soil harbored a higher proportion of genes related to reduced fungal virulence, quorum sensing, biofilm formation, and production of antimicrobial compounds. *Pseudomonas* was identified as a potential key taxon in disease suppression. *Pseudomonas* had

a higher relative abundance in suppressive soils, and *Pseudomonas* isolates recovered from disease-suppressive fields showed a higher proportion of antagonistic activity against the pathogen as compared to those recovered from conducive soils. Despite differences in location, edaphic factors, and other microbial components of the soil community across banana cropping sites examined, we were able to detect common microbiome features related to disease suppression.

## 4. Methods

**4.1. Field Production Survey and Basic Information of the Selected Orchards.** In August 2014, a field production survey of large-scale orchards (>10 ha) was performed to detect soils suppressive to *Fusarium* wilt among the main banana plantations on Hainan Island, an important banana production area in China, where topical climatic conditions dictate spring banana harvests. To minimize the effects of cultivar, cropping year, growing period, and microclimate at each site, only banana orchards suppressive and adjacent ones conducive to *Fusarium* wilt that had been planted during the same year with the same susceptible cultivar (*Musa acuminata* Cavendish cv. Brazil) were selected for this study. Typically, a maximum disease incidence of less than 15% can be tolerated by growers when considering both the economic loss and acceptability for a subsequent crop. Therefore, orchards maintaining a disease incidence lower than 15% over long-term monoculture could be considered potentially suppressive to *Fusarium* wilt. Colocated orchards with serious *Fusarium* wilt incidences were considered as disease conducive soils. At the time of the study, six pair-located orchards monocropped over 10 years and potentially suppressive (disease incidence < 15%) or conducive (disease incidence > 50%) to *Fusarium* wilt at harvest were identified in the main banana production areas on Hainan Island.

Paired potentially suppressive and colocated conducive orchards from sites 1 and 2 were located in the southwest of Hainan Island, where typical tropical monsoon climate conditions prevail with an annual temperature (AT) of about 24°C and annual precipitation (AP) of 1150 mm on average. Orchards from sites 3 to 6 were located in the northwest of Hainan Island that experience a mean AT of 23°C and AP of 2250 mm. The planting density for orchards located in southwestern Hainan Island was approximately 2,550 plants per ha and approximately 1,950 plants per ha for orchards in the northwestern region. For colocated orchards suppressive or conducive to *Fusarium* wilt, the pesticide managements and irrigations were roughly similar based on the farm records. Worth to mention, disease-suppressive orchards were usually amended with more organic fertilizer. Detailed information about these six pair-located orchards is provided in Table S1.

**4.2. Assay of *Fusarium* Wilt Incidence and Collection of Soil Samples.** *Fusarium* wilt incidence was monitored according to observation of typical wilt symptoms [53]. Three representative subplots (50 m × 40 m, long × width) within each field were randomly divided for soil samples collection and disease incidence estimation in August, 2014, at the banana harvest stage. *Fusarium* wilt incidence was calculated as the proportion of infected plants among the total number of bananas planted. In each subplot, five banana trees without wilt symptoms were chosen for soil sampling according to the previously described method [54]. In total, eighteen soils from disease-suppressive orchard and eighteen soils from colocated orchards were sampled for further analysis. After removing the plant residues in soil, half of each soil sample was air-dried for chemical property measurements, and the remainder was mixed with glycerin and stored at -80°C for subsequent microbial analysis and isolation of bacterial strains.

**4.3. Determination of Soil Chemical Properties and Extraction of Soil Genomic DNA.** Soil chemical properties including soil pH, content of available phosphorus (AP), available potassium (AK), total carbon (TOC), total nitrogen (TON), ammonium nitrogen (NH<sub>4</sub><sup>+</sup>-N), nitrate nitrogen (NO<sub>3</sub><sup>-</sup>-N), electrical conductivity (EC), and total carbon-nitrogen ratio (C/N) were determined according to the previously described method [55]. Soil genomic DNA was extracted by using the DNeasy® PowerSoil® Kit (QIAGEN GmbH, Germany), following the manufacturer's instructions.

**4.4. Quantification of Bacteria, Fungi, and *Foc4* Abundance.** Abundances of bacteria, fungi, and *Foc4* were measured using a 7500 Real Time PCR System (Applied Biosystems, USA) following the established protocols with the primers of Eub338F/Eub518R for bacteria, ITS1f/5.8s for fungi, and *FocSc-1*/*FocSc-2* for *Foc4*, respectively, [56, 57]. Tenfold serial dilutions of plasmids containing a full-length copy of the 16S rRNA gene from *Escherichia coli*, the 18S rRNA gene from *Saccharomyces cerevisiae*, and a fragment copy of the internal transcribed spacer (ITS) from *Foc4*, respectively, were used to generate standard curves. The *Foc4* strain, with which the pathogenicity to banana was tested [58], was provided by our own lab. Quantitative PCR amplification for

standard and DNA samples was performed in 8-well tubes with a 20 µl mixture for each reaction using SYBR®Premix Ex Taq™ (TaKaRa, Japan). Each PCR reaction contained 2 µl target DNA, 10 µl SYBR Green Premix Ex Taq (2 ×), 0.4 µl of each primer, 0.4 µl ROX Reference Dye II, and sterilized water. Thermal cycling conditions for each sample were conducted according to a standard procedure with three replicates, and the results were expressed as log copy numbers g<sup>-1</sup> dry soil.

**4.5. Construction and Sequencing of Amplicon Sequencing Library.** Bacterial and fungal sequencing libraries were built following the previously established protocols [59, 60]. The V4 region of bacterial 16S rRNA genes and the internal transcribed spacer 1 region (ITS1) were amplified using the primers of 515F/806R and ITS1F/ITS2, respectively. Amplicon qualities and concentrations were assessed by an Agilent 2100 Bioanalyzer Instrument (Agilent Technologies Co. Ltd, USA) and a KAPA Library Quantification Kit (KapaBiosystems, USA). Illumina HiSeq 2000 was used to sequence all constructed libraries at the Novogene Bioinformatics Institute (Beijing, China).

**4.6. Processing of DNA Sequence Data.** Raw DNA sequences with about 300 bp were split to each sample based on the unique barcodes and trimmed of the adaptor and primer sequences in QIIME (v. 1.2.0) and USEARCH (v. 9.1.13) [61]. OTU clustering was performed based on 97% pairwise identity with filtering the chimeras using the UPARSE algorithm after quality control and removal of archaea sequences [62]. The mitochondrial and nonbacterial OTUs together with OTUs whose relative abundance was lower than 0.01% were further removed. The affiliation of representative sequence for each OTU was classified against the RDP Bacterial 16S database or the UNITE Fungal ITS database using the RDP classifier (RDP, version 11.5) [63]. OTUs with occurrence frequencies higher than 80% in all conducive or suppressive soils were selected as “core OTUs” according to a previously describe method [64]. Core bacterial and fungal OTUs in conducive or suppressive soils were identified and pooled together for subsequent analysis.

The final OTU table for whole and core microbiomes was normalized using the cumulative sum scaling method [65]. Nonmetric multidimensional scaling ordination analysis was performed using the weighted UniFrac distances and was plotted using “scatterplot3d” (v. 0.3-12) in R 3.1.2. The significant differences of bacterial or fungal composition between disease suppressive and conducive soils were tested using the code of “adonis” in the R 3.1.2 “vegan” package (v. 2.6-2). Venn diagrams were then plotted to dissect microbial community composition in disease-suppressive and -conductive soils based on the all and core OTU datasets.

**4.7. Taxonomic Analysis of the Core Microbiome.** To compare the differences in taxonomic composition and to assess whether some bacterial taxa were differentially abundant in the core microbiome across samples, a three-step analysis was conducted in which the read counts were assessed separately at the phylum, order, and genus levels according to the

previously described method [66]. Log<sub>2</sub> transformed relative changes of affiliated phyla or orders in disease-suppressive soils relative to conducive soils were calculated with FDR adjusted *p* value to compare the differences in the composition of bacterial community across disease suppressive and conducive soils and plotted using the R 3.1.2 “ggplot2” package (v. 2.2.0). The predictors of key genera within significantly enriched orders for explaining the abundance of Foc4 in disease-conductive and -suppressive soils were identified by random forest regression analysis [67].

**4.8. Quantification of *Pseudomonas* Abundance.** Abundances of *Pseudomonas* were determined with the primers *Pse435F/Pse686R* following an established protocol by a 7500 Real Time PCR System [68]. Tenfold serial dilutions of plasmids containing a full-length copy of the 16S rRNA gene from *P. putida* were used to generate standard curves. Quantitative PCR amplification for standard and DNA samples was performed in 8-well tubes with a 20  $\mu$ l mixture for each reaction using SYBR®Premix Ex Taq™ (TaKaRa, Japan). Each PCR reaction contained 2  $\mu$ l target DNA, 10  $\mu$ l SYBR Green Premix Ex Taq (2  $\times$ ), 0.4  $\mu$ l of each primer, 0.4  $\mu$ l ROX Reference Dye II, and sterilized water. Thermal cycling conditions for each sample were conducted according to a standard procedure with three replicates, and the results were expressed as log copy numbers g<sup>-1</sup> dry soil.

**4.9. Greenhouse Assay of Soil Suppressiveness to Banana *Fusarium* Wilt.** Subplots from pair-located orchards at site 3 were randomly selected at harvest to validate the soil suppressiveness phenomenon. Topsoil to a depth of 30 cm from the conducive and suppressive orchards was collected in October, 2014. This soil was used in a pot experiment to investigate the activity of disease-suppressive soil against Foc4 invasion. Four treatments with four replicates each were designed: (1) C, conducive soil without Foc4 inoculation; (2) CF, conducive soil inoculated with Foc4; (3) S, suppressive soil without Foc4 inoculation; and (4) SF, suppressive soil inoculated with Foc4. A total of eighteen pots, resulting in five or four pots each replicates, were set up for each treatment, and each pot was loaded with 4.5 kg dry soil and sown with one tissue-cultured banana seedling (*M. acuminata* Cavendish cv. Brazil). All pots were randomly placed and managed under the same conditions in the greenhouse. Two months later, pathogenic conidia of Foc4 in sterile water were added to the CF and SF treatments to give a final conidial density of 2  $\times$  10<sup>4</sup> dry weight in soil while the same volume of sterile water was irrigated into the C and S treatments. To prepare conidia, an 8 mm plug from the leading edge of a 7-day-old culture of Foc4 on potato dextrose agar medium (PDA) was placed onto the center of a fresh PDA plate, then cultured at 28 °C for 7 days, after which 5 ml sterile water was added and through four layers gauze to harvest spores. The number of spores was estimated by a hemocytometer. Then, the same number of pathogen spores was added again to the treatments one month later. After the harvest of the first season, the second season was planted immediately, and the operation was the same as that of the first season; we here use the disease incidence of the second season.

Meanwhile, four treatments with three replicates each were designed for another greenhouse experiment as follows: (1) C, soil from the orchard conducive to *Fusarium* wilt; (2) S, soil from the orchard suppressive to *Fusarium* wilt; (3) CS, soil from the orchard conducive to *Fusarium* wilt mixed with disease-suppressive soil at a ratio of 9:1 (v/v); and (4) S50, soil from the orchard suppressive to *Fusarium* wilt was heated at 50°C in an oven for 2 h. Each replicate comprised ten pots while each pot was loaded with 6 kg soil and sown with one tissue-cultured banana seedling. All pots were randomly placed and managed under the same condition in the greenhouse. Symptoms of *Fusarium* wilt were monitored weekly after transplantation, and disease incidence was calculated as described above.

**4.10. Metagenomic Sequencing of Disease-Suppressive Soil and Microbial Function Analysis.** Soil from the banana orchard at site 3 and the collocated conducive orchard were selected for further metagenomic sequencing in August 2015 at the harvest stage. Five representative subplots of 50 m  $\times$  40 m from each orchard were sampled. Within each subplot, fifteen soil cores under the trunk base from five separate banana trees without wilt symptoms were sampled and pooled as a composite sample. Genomic DNA of 5 g soil from each replicate was extracted with the PowerMax®Soil DNA Isolation kit (MoBio Laboratories Inc., USA) and prepared for sequencing as described in the Illumina Paired-End Prep kit protocol. The extracted DNA was fragmented to a mean size of about 300 bp using Covaris M220 (Gene Company Limited, China), and paired-end libraries were then constructed with TruSeq™ DNA Sample Prep Kits (Illumina, San Diego, CA, USA). Adapters containing the full complement of sequencing primer hybridization sites were ligated to the blunt-ends of all fragments. Shotgun sequencing was performed on an Illumina HiSeq 4000 platform (Illumina Inc., San Diego, CA, USA) at Majorbio Bio-Pharm Technology Co., Ltd. (Shanghai, China).

The SeqPrep software (<https://github.com/jstjohn/SeqPrep>) was firstly used to remove the adapter sequences, and the library sickle (<https://github.com/najoshi/sickle>) was then used to trim the reads. If the mean quality of bases inside a window dropped below 20, the remainder of the read below the quality threshold was trimmed. Quality-trimmer reads shorter than 50 bp or containing ambiguous bases were also discarded. The filtered sequences were de novo assembled using SOAP software (<http://soap.genomics.org.cn>, V. 1.06). The *k*-mer value of the main splicing parameter was set in the range of 39-47. Prediction of genes of the assembled contigs to open reading frames (ORFs) was performed using MetaGene software. All of the predicted gene sequences were clustered using CD-HIT software (v. 4.6.4). Further, the longest gene was used as a representative sequence for each cluster to construct a nonredundant gene set. The high-quality reads of each sample were matched to the nonredundant gene set (95% identity) using SOAPaligner software to build a comprehensive metagenome reference gene set for further analysis. The composition difference of functions was compared based on this final gene set by conducting NMDS ordinations in the R 3.1.2 “vegan” package

(v. 2.6-2). First, the final metagenome reference gene set was blasted using BLASTP against the NCBI nr database (June 2020) to obtain the taxonomic assignment. Then, the annotation of the gene set was blasted using BLASTP against the egg-nog database to obtain Clusters of Orthologous Groups (COG) (2003 COGs, 2014 update), and against the Kyoto Encyclopedia of Genes and Genomes (KEGG) database (Release 95.2) to obtain the pathway information for genes. The annotation of the gene set was blasted using BLASTP against pathogen-host interaction (PHI) databases (v. 4.10) to obtain the functions related to pathogen and host interaction. Furthermore, the contigs with length larger than 5 kb were processed with antiSMASH (V. 5.0) with default parameters to analyze the secondary metabolism ability according to the previously described method [69].

**4.11. Determinations of Total Culturable Bacterial Counts, Recovery of *Pseudomonas* Isolates, and In Vitro Tests of Antagonistic Activity against *Foc4*.** Considering *Pseudomonas* was identified as a key specie in maintaining soil suppressiveness based on high-throughput sequencing analysis, culturable *Pseudomonas* was isolated. Five grams of the collected soil from six pair-located disease-suppressive and -conductive orchards which was mixed with glycerin and stored at  $-80^{\circ}\text{C}$  previously was added to a 150 mL Erlenmeyer flask containing 45 mL of sterilized distilled water. After shaken for 30 min at 170 rpm at  $30^{\circ}\text{C}$ , 10-fold serial dilutions were made, and appropriate suspensions were loaded onto Tryptic Soy Broth with one-tenth-strength ( $1/10$  TSB) to determine total culturable heterotrophic bacterial counts. Similarly, the same dilution series was spread onto King's medium B (KB) to enumerate culturable *Pseudomonas* and recover *Pseudomonas* isolates. All culture plates were incubated for 36 h at  $30^{\circ}\text{C}$ . Forty colonies from the KB plates for each soil sample were randomly picked to isolate potential antagonists against the *Foc4* on the PDA medium using the dual culture method [70]. Isolates showing the antagonistic zones were further cultured in KB broth, and genomic DNA was then extracted using a rapid one-tube genomic DNA extraction protocol [71]. The bacterial 16S rRNA genes were amplified using the primer 27F/1492R to generate phylogenetic information.

**4.12. Evaluating the Biocontrol Activity of Isolated *Pseudomonas* Strains.** The effects of four *Pseudomonas* isolates showing the strongest antagonistic activity in disease-suppressive soils against banana *Fusarium* wilt were further assessed in the greenhouse of WanZhong Agricultural Company from March to May, 2016. The topsoil from conducive orchards to *Fusarium* wilt at site 3 was collected for this biocontrol test. Five treatments with three replicates each were established including conducive soil amended with 50 mL fermentation culture of the *Pseudomonas* strains S9 (T1), S20 (T2), S27 (T3), S40 (T4), and equally mixed fermentation culture from all above four strains (T5). Monocropped soil amended with 50 mL sterile KB broth (CK) was included as a control. Each replicate contained ten pots, transplanted with a single tissue-cultured banana seedling. The fermenta-

tion liquor of the various strains was added into soil near the pseudostem at weekly intervals beginning 15 days after the seedlings had been transplanted. After three months, *Fusarium* wilt was monitored weekly and measured as above.

**4.13. Determinations of the Abundance of *Pseudomonas* and *F. oxysporum* in the Soil Amended with Isolated *Pseudomonas* Strains.** Rhizosphere soil was sampled in May, 2016 from three banana plants without obvious infection symptoms. All roots from the replicates were pooled, then shaken gently by hand to remove the loosely adhered soil, and minced into fragments approximately 5 cm long. For each sample, about 200 g of roots were placed into a 500 mL Erlenmeyer flask previously loaded with 200 mL of sterilize distilled water. After shaken at 170 rpm for 30 min at ambient temperature, the roots were removed, and the soil slurry were then centrifuged at  $4000\times g$  for 5 min. The plant residue was carefully removed by sterilized tweezers, genomic DNA in the sediment soil was extracted, and then the abundance of *F. oxysporum* and *Pseudomonas* was determined.

## Data Availability

Raw amplicon sequencing data was deposited at the National Center for Biotechnology Information (NCBI) under the accession number of PRJNA627608. All shotgun raw sequences were stored at NCBI with the accession number of PRJNA630300. The 16S rRNA gene sequences of four *Pseudomonas* isolates were deposited in the GenBank database under accession numbers MT364444-MT364447.

## Conflicts of Interest

The authors declare that they have no competing interests.

## Authors' Contributions

Z. Shen performed all experiments. Z. Shen, R. Li, Q. Shen, and G. A. Kowalchuk designed the study and wrote the majority of the manuscript. Z. Shen and C. Tao analyzed the data. L. S. Thomashow, W. Xiong, C. Tao, J. Wang, and G. A. Kowalchuk participated in the design of the study, provided comments, and edited the manuscript. The authors read and approved the final manuscript.

## Acknowledgments

We thank Chun Luo from Majorbio Bio-Pharm Technology Co., Ltd. (Shanghai, China) for helping us dealing with the metagenomics data. This research was supported by the National Natural Science Foundation of China (31972509, 42090065, and 42107142) and the Guidance Foundation of the Sanya Institute of Nanjing Agricultural University (NAUSY-MS10).

## Supplementary Materials

Figure S1: violin plot showing abundance of total bacteria and fungi and ratio of bacteria to fungi (*B/F*) in disease conducive (*C*) and suppressive (*S*) soils determined by qPCR.

The  $p$  values in the plot were calculated based on Wilcoxon test and corrected by FDR. Figure S2: the rarefaction curves for whole bacterial and fungal communities in disease conducive (C) and suppressive (S) soils. C1-18 with pink color represent subsamples for conducive soil collected from site 1 to site 6 while S1-18 with cyan color represent subsamples for suppressive soil collected from site 1 to site 6. Figure S3: violin plot showing Shannon index of core bacterial and fungal communities in disease-conducive (C) and -suppressive (S) soils. Figure S4: stacked bar chart depicting the distribution of dominant phyla in core bacterial and fungal communities. C1-18 represent subsamples for conducive soil collected from site 1 to site 6 while S1-18 represent subsamples for suppressive soil collected from site 1 to site 6. Figure S5: violin plot showing relative abundance of five key genera which were significantly enriched in disease-suppressive soils among Myxococcales, Pseudomonadales, and Xanthomonadales. The  $p$  values in the plot were calculated based on Wilcoxon test and corrected by FDR. Table S1: field site information and soil chemical properties of sampled soils. C and S indicate that the soil samples were collected from orchards conducive or suppressive to banana *Fusarium* wilt, respectively. Symbol \* presents a significant difference for mean value of each soil chemical property observed between all conducive and suppressive soils based on corrected Wilcoxon test. TON represents content of soil total nitrogen, TOC represents content of soil total carbon,  $\text{NH}_4^+$ -N indicates content of soil ammonium nitrogen,  $\text{NO}_3^-$ -N represents content of soil nitrate nitrogen, EC represents soil electrical conductivity, AP represents content of soil available phosphorus, AK represents content of soil available potassium, and C/N represents ratio of soil total carbon to total nitrogen. Table S2: general information of sequencing data used for final analysis after basic quality control for whole and core microbiomes. Table S3: PERMANOVA results for whole and core bacterial and fungal community structures at the OTU level.  $p$  values were calculated based on 999 permutations (lowest  $p$  value possible is 0.001). Site means location of sampled soils, and suppression ability indicates the soils conducive or suppressive to banana *Fusarium* wilt. Table S4: relative abundance of phylum for core bacterial and fungal community in disease-conducive (C) and -suppressive (S) soils. Table S5: relative abundance of dominate orders within Proteobacteria for the core bacterial community in disease-conducive (C) and -suppressive (S) soils. Table S6: overview of sequences of shotgun-metagenome datasets representing each soil sample. Table S7: overview of genes catalog assembly to open reading frames (ORFs) (*Supplementary Materials*). (*Supplementary Materials*)

## References

- [1] M. Delgado-Baquerizo, C. A. Guerra, C. Cano-Díaz et al., "The proportion of soil-borne pathogens increases with warming at the global scale," *Nature Climate Change*, vol. 10, no. 6, pp. 550–554, 2020.
- [2] R. N. Strange and P. R. Scott, "Plant disease: a threat to global food security," *Annual Review of Phytopathology*, vol. 43, no. 1, pp. 83–116, 2005.
- [3] J. Yuan, T. Wen, H. Zhang et al., "Predicting disease occurrence with high accuracy based on soil macroecological patterns of *Fusarium* wilt," *The ISME Journal*, vol. 14, no. 12, pp. 2936–2950, 2020.
- [4] D. Butler, "Fungus threatens top banana: fears rise for Latin American industry as devastating disease hits leading variety in Africa and Middle East," *Nature*, vol. 504, no. 7479, pp. 195–196, 2013.
- [5] R. C. Ploetz, "Fusarium wilt of banana," *Phytopathology*, vol. 105, no. 12, pp. 1512–1521, 2015.
- [6] R. L. Berendsen, C. M. Pieterse, and P. A. H. M. Bakker, "The rhizosphere microbiome and plant health," *Trends in Plant Science*, vol. 17, no. 8, pp. 478–486, 2012.
- [7] G. Bubici, M. Kaushal, M. I. Prigigallo, C. G. Cabanás, and J. Mercado-Blanco, "Biological control agents against *Fusarium* wilt of banana," *Frontiers in Microbiology*, vol. 10, p. 616, 2019.
- [8] R. J. Cook and A. D. Rovira, "The role of bacteria in the biological control of *Gaeumannomyces graminis* by suppressive soils," *Soil Biology and Biochemistry*, vol. 8, no. 4, pp. 269–273, 1976.
- [9] J. Y. Cha, S. Han, H. J. Hong et al., "Microbial and biochemical basis of a *Fusarium* wilt-suppressive soil," *The ISME Journal*, vol. 10, pp. 119–129, 2016.
- [10] R. Mendes, M. Kruijt, I. De Bruijn et al., "Deciphering the rhizosphere microbiome for disease-suppressive bacteria," *Science*, vol. 332, no. 6033, pp. 1097–1100, 2011.
- [11] M. Kyselková, J. Kopecký, M. Frapolli et al., "Comparison of rhizobacterial community composition in soil suppressive or conducive to tobacco black root rot disease," *The ISME Journal*, vol. 3, no. 10, pp. 1127–1138, 2009.
- [12] H. Sanguin, A. Sarniguet, K. Gazengel, Y. Moënné-Loccoz, and G. L. Grundmann, "Rhizosphere bacterial communities associated with disease suppressiveness stages of take-all decline in wheat monoculture," *New Phytologist*, vol. 184, no. 3, pp. 694–707, 2009.
- [13] J. Dominguez, M. A. Negrin, and C. M. Rodriguez, "Evaluating soil sodium indices in soils of volcanic nature conducive or suppressive to *Fusarium* wilt of banana," *Soil Biology and Biochemistry*, vol. 35, no. 4, pp. 565–575, 2003.
- [14] P. Deltour, S. C. França, O. L. Pereira et al., "Disease suppressiveness to *Fusarium* wilt of banana in an agroforestry system: Influence of soil characteristics and plant community," *Agriculture, ecosystems & environment*, vol. 239, pp. 173–181, 2017.
- [15] Z. Shen, Y. Ruan, C. Xue, S. Zhong, R. Li, and Q. Shen, "Soils naturally suppressive to banana *Fusarium* wilt disease harbor unique bacterial communities," *Plant and Soil*, vol. 393, no. 1–2, pp. 21–33, 2015.
- [16] D. Schlatter, L. Kinkel, L. S. Thomashow, D. M. Weller, and T. Paulitz, "Disease suppressive soils: new insights from the soil microbiome," *Phytopathology*, vol. 107, no. 11, pp. 1284–1297, 2017.
- [17] R. G. Expósito, J. Postma, J. M. Raaijmakers, and I. D. Bruijn, "Diversity and activity of *Lysobacter* species from disease suppressive soils," *Frontiers in Microbiology*, vol. 6, p. 1243, 2015.
- [18] V. J. Carrión, V. Cordovez, O. Tyc et al., "Involvement of Burkholderiaceae and sulfurous volatiles in disease-suppressive soils," *The ISME Journal*, vol. 12, no. 9, pp. 2307–2321, 2018.
- [19] E. Coller, A. Cestaro, R. Zanzotti et al., "Microbiome of vineyard soils is shaped by geography and management," *Microbiome*, vol. 7, no. 1, pp. 1–5, 2019.

- [20] P. Trivedi, J. E. Leach, S. G. Tringe, T. Sa, and B. K. Singh, "Plant-microbiome interactions: from community assembly to plant health," *Nature Reviews Microbiology*, vol. 18, no. 11, pp. 607–621, 2020.
- [21] J. M. Raaijmakers and M. Mazzola, "Soil immune responses," *Science*, vol. 352, no. 6292, pp. 1392–1393, 2016.
- [22] D. S. Lundberg, S. L. Lebeis, S. H. Paredes et al., "Defining the core *Arabidopsis thaliana* root microbiome," *Nature*, vol. 488, no. 7409, pp. 86–90, 2012.
- [23] D. Bulgarelli, M. Rott, K. Schlaeppli et al., "Revealing structure and assembly cues for *Arabidopsis* root-inhabiting bacterial microbiota," *Nature*, vol. 488, no. 7409, pp. 91–95, 2012.
- [24] D. Zhou, T. Jing, Y. Chen et al., "Deciphering microbial diversity associated with *Fusarium* wilt-diseased and disease-free banana rhizosphere soil," *BMC microbiology*, vol. 19, no. 1, pp. 1–3, 2019.
- [25] M. Kaushal, G. Mahuku, and R. Swennen, "Metagenomic insights of the root colonizing microbiome associated with symptomatic and non-symptomatic bananas in *Fusarium* wilt infected fields," *Plants*, vol. 9, no. 2, p. 263, 2020.
- [26] W. A. Walters, Z. Jin, N. Youngblut et al., "Large-scale replicated field study of maize rhizosphere identifies heritable microbes," *Proceedings of the National Academy of Sciences of the United States of America*, vol. 115, no. 28, pp. 7368–7373, 2018.
- [27] E. E. Kuramae, E. Yergeau, L. C. Wong, A. S. Pijl, J. A. van Veen, and G. A. Kowalchuk, "Soil characteristics more strongly influence soil bacterial communities than land-use type," *FEMS Microbiology Ecology*, vol. 79, no. 1, pp. 12–24, 2012.
- [28] Y. K. Yeoh, P. G. Dennis, C. Paungfoo-Lonhienne et al., "Evolutionary conservation of a core root microbiome across plant phyla along a tropical soil chronosequence," *Nature Communications*, vol. 8, no. 1, p. 215, 2017.
- [29] H. Toju, K. G. Peay, M. Yamamichi et al., "Core microbiomes for sustainable agroecosystems," *Nature Plants*, vol. 4, no. 5, pp. 247–257, 2018.
- [30] T. Cernava, A. Erlacher, J. Soh, C. W. Sensen, M. Grube, and G. Berg, "Enterobacteriaceae dominate the core microbiome and contribute to the resistome of arugula (*Eruca sativa* Mill.)," *Microbiome*, vol. 7, no. 1, p. 13, 2019.
- [31] Y. K. Yeoh, C. Paungfoo-Lonhienne, P. G. Dennis et al., "The core root microbiome of sugarcane cultivated under varying nitrogen fertilizer application," *Environmental Microbiology*, vol. 18, no. 5, pp. 1338–1351, 2016.
- [32] J. E. Pérez-Jaramillo, M. D. Hollander, C. A. Ramírez, R. Mendes, J. M. Raaijmakers, and V. J. Carrión, "Deciphering rhizosphere microbiome assembly of wild and modern common bean (*Phaseolus vulgaris*) in native and agricultural soils from Colombia," *Microbiome*, vol. 7, no. 1, p. 114, 2019.
- [33] P. E. Galand, O. Pereira, C. Hochart, J. C. Auguet, and D. Debross, "A strong link between marine microbial community composition and function challenges the idea of functional redundancy," *The ISME Journal*, vol. 12, no. 10, pp. 2470–2478, 2018.
- [34] M. Delgado-Baquerizo, F. T. Maestre, P. B. Reich et al., "Microbial diversity drives multifunctionality in terrestrial ecosystems," *Nature Communications*, vol. 7, no. 1, p. 10541, 2016.
- [35] M. G. A. van der Heijden, R. D. Bardgett, and N. M. van Straalen, "The unseen majority: soil microbes as drivers of plant diversity and productivity in terrestrial ecosystems," *Ecology Letters*, vol. 11, no. 3, pp. 296–310, 2008.
- [36] Z. Shen, C. Xue, C. R. Penton et al., "Suppression of banana Panama disease induced by soil microbiome reconstruction through an integrated agricultural strategy," *Soil Biology and Biochemistry*, vol. 128, pp. 164–174, 2019.
- [37] M. Köberl, M. Dita, A. Martinuz, C. Staver, and G. Berg, "Agroforestry leads to shifts within the gammaproteobacterial microbiome of banana plants cultivated in Central America," *Frontiers in Microbiology*, vol. 6, p. 91, 2015.
- [38] M. Köberl, M. Dita, A. Martinuz, C. Staver, and G. Berg, "Members of *Gammaproteobacteria* as indicator species of healthy banana plants on *Fusarium* wilt-infested fields in Central America," *Scientific Reports*, vol. 7, article 45378, 2017.
- [39] X. Ye, Z. Li, X. Luo et al., "A predatory myxobacterium controls cucumber *Fusarium* wilt by regulating the soil microbial community," *Microbiome*, vol. 8, no. 1, p. 49, 2020.
- [40] C. Yin, J. M. C. Vargas, D. C. Schlatter, C. H. Hagerty, S. H. Hulbert, and T. C. Paulitz, "Rhizosphere community selection reveals bacteria associated with reduced root disease," *Microbiome*, vol. 9, no. 1, p. 86, 2021.
- [41] D. Haas and G. Défago, "Biological control of soil-borne pathogens by fluorescent pseudomonads," *Nature Reviews Microbiology*, vol. 3, no. 4, pp. 307–319, 2005.
- [42] S. Mazurier, T. Corberand, P. Lemanceau, and J. M. Raaijmakers, "Phenazine antibiotics produced by fluorescent pseudomonads contribute to natural soil suppressiveness to *Fusarium* wilt," *The ISME Journal*, vol. 3, no. 8, pp. 977–991, 2009.
- [43] C. Gómez-Lama Cabanás, A. J. Fernández-González, M. Cardoni et al., "The banana root endophytome: differences between mother plants and suckers and evaluation of selected bacteria to control *Fusarium oxysporum* f.sp. cubense," *Journal of Fungi*, vol. 7, no. 3, p. 194, 2021.
- [44] C. F. Michelsen, J. Watrous, M. A. Glaring et al., "Nonribosomal peptides, key biocontrol components for *Pseudomonas fluorescens* In5, isolated from a Greenlandic suppressive soil," *MBio*, vol. 6, no. 2, article e00079, 2015.
- [45] A. Santos Kron, V. Zengerer, M. Bieri et al., "*Pseudomonas orientalis* F9 pyoverdine, safracin, and phenazine mutants remain effective antagonists against *Erwinia amylovora* in apple flowers," *Applied Environmental Microbiology*, vol. 86, no. 8, article e02620, 2020.
- [46] B. E. Ramey, M. Koutsoudis, S. B. von Bodman, and C. Fuqua, "Biofilm formation in plant-microbe associations," *Current Opinion in Microbiology*, vol. 7, no. 6, pp. 602–609, 2004.
- [47] I. S. Kim, S. Y. Yang, S. K. Park, and Y. C. Kim, "Quorum sensing is a key regulator for the antifungal and biocontrol activity of chitinase-producing *Chromobacterium* sp. C61," *Molecular Plant Pathology*, vol. 18, no. 1, pp. 134–140, 2017.
- [48] S. Mukherjee and B. L. Bassle, "Bacterial quorum sensing in complex and dynamically changing environments," *Nature Reviews Microbiology*, vol. 17, no. 6, pp. 371–382, 2019.
- [49] C. Tao, R. Li, W. Xiong et al., "Bio-organic fertilizers stimulate indigenous soil *Pseudomonas* populations to enhance plant disease suppression," *Microbiome*, vol. 8, no. 1, p. 137, 2020.
- [50] S. Louca, M. F. Polz, F. Mazel et al., "Function and functional redundancy in microbial systems," *Nature Ecology and Evolution*, vol. 2, no. 6, pp. 936–943, 2018.
- [51] V. J. Carrión, J. Perez-Jaramillo, V. Cordovez et al., "Pathogen-induced activation of disease-suppressive functions in the endophytic root microbiome," *Science*, vol. 366, no. 6465, pp. 606–612, 2019.

- [52] P. Garbeva, M. W. Silby, J. M. Raaijmakers, S. B. Levy, and W. D. Boer, "Transcriptional and antagonistic responses of *Pseudomonas fluorescens* Pf0-1 to phylogenetically different bacterial competitors," *The ISME Journal*, vol. 5, no. 6, pp. 973–985, 2011.
- [53] M. Dita, M. Barquero, D. Heck, E. S. G. Mizubuti, and C. P. Staver, "Fusarium wilt of banana: current knowledge on epidemiology and research needs toward sustainable disease management," *Frontiers in Plant Science*, vol. 9, p. 1468, 2018.
- [54] Z. Shen, C. R. Penton, N. Lv et al., "Banana *Fusarium* wilt disease incidence is influenced by shifts of soil microbial communities under different monoculture spans," *Microbial Ecology*, vol. 75, no. 3, pp. 739–750, 2018.
- [55] Z. Shen, S. Zhong, Y. Wang et al., "Induced soil microbial suppression of banana fusarium wilt disease using compost and biofertilizers to improve yield and quality," *European Journal of Soil Biology*, vol. 57, pp. 1–8, 2013.
- [56] Y. Lin, C. Su, C. Chao et al., "A molecular diagnosis method using real-time PCR for quantification and detection of *Fusarium oxysporum* f. sp. *cubense* race 4," *European Journal of Plant Pathology*, vol. 135, no. 2, pp. 395–405, 2013.
- [57] N. Fierer, J. A. Jackson, R. Vilgalys, and R. B. Jackson, "Assessment of soil microbial community structure by use of taxon-specific quantitative PCR assays," *Applied and Environmental Microbiology*, vol. 71, no. 7, pp. 4117–4120, 2005.
- [58] X. He, Q. Huang, X. Yang et al., "Screening and identification of pathogen causing banana *Fusarium* wilt and the relationship between spore suspension concentration and the incidence rate," *Scientia Agricultura Sinica*, vol. 43, no. 18, pp. 3809–3816, 2010, (in Chinese).
- [59] J. J. Kozich, S. L. Westcott, N. T. Baxter, S. K. Highlander, and P. D. Schloss, "Development of a dual-index sequencing strategy and curation pipeline for analyzing amplicon sequence data on the MiSeq Illumina sequencing platform," *Applied and Environmental Microbiology*, vol. 79, no. 17, pp. 5112–5120, 2013.
- [60] J. G. Caporaso, C. L. Lauber, W. A. Walters et al., "Global patterns of 16S rRNA diversity at a depth of millions of sequences per sample," *Proceedings of the National Academy of Sciences of the United States of America*, vol. 108, supplement\_1, pp. 4516–4522, 2011.
- [61] J. G. Caporaso, J. Kuczynski, J. Stombaugh et al., "QIIME allows analysis of high-throughput community sequencing data," *Nature Methods*, vol. 7, no. 5, pp. 335–336, 2010.
- [62] R. C. Edgar, "UPARSE: highly accurate OTU sequences from microbial amplicon reads," *Nature Methods*, vol. 10, no. 10, pp. 996–998, 2013.
- [63] Q. Wang, G. M. Garrity, J. M. Tiedje, and J. R. Cole, "Naïve Bayesian classifier for rapid assignment of rRNA sequences into the new bacterial taxonomy," *Applied and Environmental Microbiology*, vol. 73, no. 16, pp. 5261–5267, 2007.
- [64] S. Jacquiod, R. Puga-Freitas, A. Spor et al., "A core microbiota of the plant-earthworm interaction conserved across soils," *Soil Biology and Biochemistry*, vol. 144, article 107754, 2020.
- [65] J. N. Paulson, O. C. Stine, H. C. Bravo, and M. Pop, "Differential abundance analysis for microbial marker-gene surveys," *Nature Methods*, vol. 10, no. 12, pp. 1200–1202, 2013.
- [66] M. E. Ritchie, B. Phipson, D. I. Wu et al., "*limma* powers differential expression analyses for RNA-sequencing and microarray studies," *Nucleic acids research*, vol. 43, no. 7, p. e47, 2015.
- [67] L. Breiman, "Random forests," *Machine Learning*, vol. 45, no. 1, pp. 5–32, 2001.
- [68] L. Bergmark, P. H. B. Poulsen, W. A. Al-Soud, A. Norman, L. H. Hansen, and S. J. Sorensen, "Assessment of the specificity of *Burkholderia* and *Pseudomonas* qPCR assays for detection of these genera in soil using 454 pyrosequencing," *FEMS Microbiology Letters*, vol. 333, no. 1, pp. 77–84, 2012.
- [69] K. Blin, S. Shaw, K. Steinke et al., "antiSMASH 5.0: updates to the secondary metabolite genome mining pipeline," *Nucleic Acids Research*, vol. 47, no. W1, pp. W81–W87, 2019.
- [70] A. K. M. Jaaffar, J. A. Parejko, T. C. Paulitz, D. M. Weller, and L. S. Thomashow, "Sensitivity of *Rhizoctonia* Isolates to Phenazine-1-Carboxylic Acid and Biological Control by Phenazine-Producing *Pseudomonas* spp," *Phytopathology*, vol. 107, no. 6, pp. 692–703, 2017.
- [71] J. J. Steiner, C. J. Poklemba, R. G. Fjellstrom, and L. F. Elliott, "A rapid one-tube genomic DNA extraction process for PCR and RAPD analyses," *Nucleic Acids Research*, vol. 23, no. 13, pp. 2569–2570, 1995.